

## Atmospheric Moisture Recycling: Role of Advection and Local Evaporation

KEVIN E. TRENBERTH

*National Center for Atmospheric Research,\* Boulder, Colorado*

(Manuscript received 24 November 1997, in final form 16 April 1998)

### ABSTRACT

An approximate formulation of how much moisture that precipitates out comes from local evaporation versus horizontal transport, referred to as “recycling,” has allowed new estimates of recycling to be mapped globally as a function of length scale. The recycling is formulated in terms of the “intensity of the hydrological cycle”  $I$ , which is alternatively referred to as a “precipitation efficiency” as it denotes the fraction of moisture flowing through a region that is precipitated out, and a “moistening efficiency,”  $M$ , which is defined as the fraction of moisture evaporated from a region to that flowing through. While datasets of the pertinent quantities have improved, they still contain uncertainties. Results show that often the intensity is not greatest at times of greatest precipitation because moisture transport into the region is also a maximum, especially in the monsoonal regions. The annual cycle variations of  $I$  are fairly small over North America and Europe while large seasonal variations in  $M$  occur in most places. Seasonal mean maps of precipitation, evaporation ( $E$ ), and atmospheric moisture transport are presented and discussed along with the seasonal and annual means of derived precipitation and moisture efficiencies and the recycling fraction. The recycling results depend greatly on the scale of the domain under consideration and global maps of the recycling for seasonal and annual means are produced for 500- and 1000-km scales that therefore allow the heterogeneity of the fields across river basins to be captured. Global annual mean recycling for 500-km scales is 9.6%, consisting of 8.9% over land and 9.9% over the oceans. Even for 1000-km scales, less than 20% of the annual precipitation typically comes from evaporation within that domain. Over the Amazon, strong advection of moisture dominates the supply of atmospheric moisture over much of the river basin but local evaporation is much more prominent over the southern parts, and, for the annual cycle as a whole, about 34% of the moisture is recycled. Over the Mississippi Basin, the recycling is about 21%. The smaller number mostly reflects the smaller domain size. Relatively high annual values of recycling (>20%) occur in the subtropical highs, where  $E$  is high and the advective moisture flux is small, and in convergence zones where, again, the advective moisture flux is small. Low annual values occur over the southern oceans, the North Pacific, and the eastern equatorial Pacific, where the moisture flux is at a maximum.

### 1. Introduction

There is considerable interest in the hydrology community over how changes in land use may affect the precipitation and moisture availability. The contribution of local evaporation, which could be altered by changes in land surface characteristics, to local precipitation, called “recycling,” is therefore of considerable interest. More specifically, within a catchment basin, the precipitation that falls out of the atmosphere comes from one of three sources: the moisture already in the atmosphere, convergence of the moisture advected into the region by the winds, or the evaporation of surface moisture into the atmosphere within the basin. In a steady state

or over a long period, the first is not viable and can contribute little, and so the only alternatives are evaporation and advection.

Trenberth (1998) examined the cycling times of moisture into and out of the atmosphere, referred to as “moistening,” or “restoration,” and “drying,” or “depletion” rates. The latter depend on the atmospheric moisture content and the rates by which moisture is either restored by evaporation or depleted by precipitation. They are determined by comparing local values of precipitable water,  $w$ , with the sinks of precipitation  $P$  and sources of evapotranspiration,  $E$ , and, thus, they neglect the role of advection of moisture. However, they are of interest for giving some idea of atmospheric moisture lifetimes. Overall, the  $e$ -folding residence time for atmospheric global moisture is 8.1 days for precipitation depletion and 8.5 days for evaporative restoration of atmospheric moisture. These values are computed from the global means of the inverse time constants, and the discrepancy may partly be spurious because the rates were determined using different sources of  $P$  and  $E$  data, which do not quite balance globally, but they mostly

\* The National Center for Atmospheric Research is sponsored by the National Science Foundation.

Corresponding author address: Dr. Kevin E. Trenberth, NCAR, P.O. Box 3000, Boulder, CO 80307-3000.  
E-mail: trenbert@ncar.ucar.edu

reflect real differences owing to the heterogeneous  $P$  distribution and spatial correlation with  $w$ . Only if the time constants are computed from the global means of the fields should there be a balance. In locations where  $P$  or  $E$  is very small, the implied time constants are very long. For precipitation, local values of the depletion rate are about 1 week in the tropical convergence zones, but they exceed a month in the dry zones in the subtropics and desert areas, and the pattern resembles that of the  $P$  field. The restoration rate is largest over northern Africa and in a region extending across to Saudi Arabia and Iran, and over Australia. Values average about 12 days in the tropical convergence zones and are lowest in the subtropical highs where evaporation is a maximum, but precipitable water is limited because moisture is trapped at low levels by subsidence. However, all of these values are of somewhat limited interest because they fail to take moisture transport into account.

Evaporation as a source for precipitation over land depends on the availability of surface moisture, which in turn depends upon the disposition of precipitation once it hits the ground. In particular, the latter is determined by how much infiltrates to perhaps become ground water, how much runs off into streams and rivers and is therefore effectively lost to the region as a source for further evaporation, and how much is retained near the surface in ponds, lakes, or soil moisture and is thus readily available for evapotranspiration either directly from the surface or via surface vegetation. This partitioning thus depends greatly on the surface characteristics and vegetation.

Transport of moisture into a region where it can become entrained into a precipitating weather system depends on the atmospheric dynamics as well as the sources of moisture from other parts of the globe. Of course, in some regions the atmospheric moisture is not precipitated and just flows across, while in other areas convergence of the moisture in weather systems ensures that precipitation occurs. The atmospheric branch of the hydrological cycle is therefore of considerable interest, although not as well known as is desired. Many of the same processes that are of interest over river basins also operate over the oceans. A key difference over the oceans, however, is that evaporation does not depend at all on the surface moisture budget, as the surface is always wet. Nevertheless, it is also possible to compute recycling over the oceans although, clearly, the moisture is not really being recycled.

Recycling, as defined, refers to how much evaporation in an area contributes to the precipitation in the same area. As the area is reduced to a point, the evaporation contribution tends to zero and all the moisture precipitated is transported in. At the other extreme, as the domain becomes global, the evaporation entirely replaces the precipitation. Thus, the recycling ranges from 0 to 1 depending on the size of the area. Eltahir and Bras (1996) review estimates of precipitation recycling, and Eltahir and Bras (1994) estimate that 25%–

35% of the rain that falls in the Amazon Basin is contributed by evaporation within the basin (over scales of 2500 km). In the Mississippi Basin the recycling estimates range from 10% to 24% over about 1500-km scales.

One substantial difficulty in determining recycling has been in defining the edges of a catchment basin or area of interest and determining the fluxes of moisture into and out of the region. Moreover, as each basin has a different configuration, the interpretation of the comparison of results has not been very clear. Because recycling generally increases as the size of the domain increases it does not readily translate into information on the underlying physical processes. In this paper, the difficulty is addressed by making some approximations (section 4) that allow mapping of a recycling ratio and computation of values at every point as a function of length scale. This has the distinct advantage of allowing different areas to be directly compared for each length scale.

Computation of recycling empirically requires assumptions that suggest that the results should not be taken too literally. In particular, for a given domain over a period such as a month, it is assumed that the moisture advected into the region is uniformly mixed with that from local evaporation while ignoring changes in atmospheric precipitable water so that this provides a basis for partitioning the rainfall into the average advective versus evaporative contributions. Further, this approach assumes that the overall flux of moisture is represented by the monthly or longer-term mean. While the computed flux does include contributions from both transients and the mean flow, the temporal variability of the flux within the month, such as in its direction, is not included and seems difficult to accommodate. A test of nonlinearity has been made by comparing the results for a season with those obtained over 15-day and monthly timescales, averaged over the season. The effects are small and the patterns do not change, but they are systematic in that monthly values give 6% larger estimates, primarily owing to variability in precipitation. It may therefore be more appropriate to think of these results as providing an index of recycling that should not be taken too literally but that does allow different regions of the globe to be compared under the assumptions made.

Along the way, several other indices or measures of the vigor of the hydrological cycle and the relative importance of advective versus surface fluxes are computed. Thus, an examination is made of the “intensity of the hydrological cycle” (Drozdov and Grigor’eva 1965), although a more descriptive term might be the “precipitation efficiency,” which is the fraction of moisture flowing overhead that is precipitated out. The latter term is already used in thunderstorm literature with a slightly different meaning. There precipitation efficiency is defined as the ratio of the water mass precipitated to the mass of water vapor entering the storm through

its base (e.g., Fankhauser 1988) or, in modeling studies, the ratio of total rainfall to total condensation (e.g., Ferrer et al. 1996). Similarly, we can define a “moistening efficiency” as the fraction of moisture added to that flowing overhead.

A continuing problem with determination of all of these ratios has been the availability of datasets needed to accurately compute the fields on which they are based. The sources and sinks of atmospheric moisture are evaporation and precipitation. Even climatological values are quite uncertain for both fields. Time series of monthly means globally are only now just becoming available but they require evaluation to ascertain their accuracy and usefulness. Although not without their problems, new global precipitation datasets and also analyses (the reanalyses) from the National Centers for Environmental Prediction (NCEP) using data from the National Center for Atmospheric Research (Kalnay et al. 1996) allow estimates to be made of the quantities of interest.

A discussion of the datasets used is given in section 2. Section 3 provides a brief description of the basic precipitation, evaporation, and atmospheric moisture transport fields, and section 4 presents the new formulation of the atmospheric moisture recycling. The results are presented and discussed in section 5.

## 2. Datasets

One source of precipitation data that is newly available is from the Global Precipitation Climatology Project (Huffman et al. 1997), for the period after 1987; these are modified somewhat and extended to cover the period after 1979 by Arkin and Xie (1994) and Xie and Arkin (1996, 1997) and are called the Climate Prediction Center Merged Analysis of Precipitation (CMAP). Over land these fields are mainly based on information from rain gauge observations, while over the ocean they primarily use satellite estimates made with several different algorithms based on outgoing longwave radiation, and scattering and emission of microwave radiation.

Another source is from the NCEP–NCAR reanalyses produced with four-dimensional data assimilation on model (sigma) surfaces with T62 spectral resolution and 28 levels in the vertical, with five of those levels in the atmospheric boundary layer; these also provide estimates of the evaporation and moisture transport. The data used are all from the averages of analyses four times daily (which captures most of the diurnal cycle) from 1979 to 1995, and fields are integrated vertically at full resolution in model coordinates. An evaluation of the NCEP moisture fields  $P$  and  $E$ , and the moisture transport and divergence in the atmosphere has been carried out by Trenberth and Guillemot (1996, 1998). The precipitable water  $w$  was compared with analyzed fields from National Aeronautics and Space Administration (NASA) Water Vapor Project (NVAP) (Randel et al. 1996), based primarily on Special Sensor Microwave/Imager (SSM/I) measurements over the oceans

and rawinsonde measurements over land, plus the Television Infrared Observation Satellite Operational Vertical Sounder. The moisture budgets were evaluated through computation of the freshwater flux at the surface  $E - P$  using residual techniques from the divergence of the total moisture transport, and this was compared with the reanalysis  $E - P$  that is based upon a 6-h integration of the assimilating model and thus depends on the model parameterizations. The  $P$  field was evaluated using Xie–Arkin CMAP estimates and, although it contains considerable uncertainties (Xie and Arkin 1997), the patterns are believed to be adequate for this purpose.

The NCEP moisture fields contain significant biases in the Tropics, the tropical structures are less well defined than the SSM/I fields, and there is an underestimate of the variability from year to year. The NCEP model  $P$  generally reveals a pronounced double intertropical convergence zone in the central Pacific and the location of the South Pacific convergence zone is not well captured. Rainfall amounts are lower than observed in the oceanic tropical convergence zones. The variability in the central tropical Pacific of  $P$  associated with El Niño–Southern Oscillation is underestimated in the NCEP reanalyses and, moreover, is not very well correlated with the CMAP product. A bias for too much rainfall in the model over the southeastern United States and southeast Asia is also present in northern summer. The comparison of  $E - P$  from the moisture budget with the model results reveals some strong systematic differences. Biases in  $E$  are inferred in some places from the  $E - P$  differences, and they probably arise from spurious land moisture sources in some cases.

Therefore, use is made of the monthly CMAP fields of precipitation from Xie and Arkin, precipitable water  $w$  from NVAP, and, in spite of the deficiencies noted above,  $E$  and moisture transport values from the NCEP reanalyses. These are adequate for current purposes, although quantitative details should be viewed with caution. Locally, values cannot be trusted because of biases in the reanalyses, but the fields are nevertheless better globally than anything previously available for this purpose. The conclusions to be drawn are believed to be robust to the data uncertainties, although quantitative details will change.

## 3. Atmospheric moisture sources and sinks

The seasonal mean precipitation CMAP  $P$  fields for 1979–95 are shown in Fig. 1. The dominant features seen on the global scale are the major tropical convergence zones and the monsoon rains over the tropical continents and maritime Asian–Australian region. These maps show the main variations in storm tracks over the extratropical oceans but the contour interval is insufficient to detail changes of significance over most land areas. Of note are the fairly sharp gradients and distinctive structures. The evaporation field (Fig. 2) also

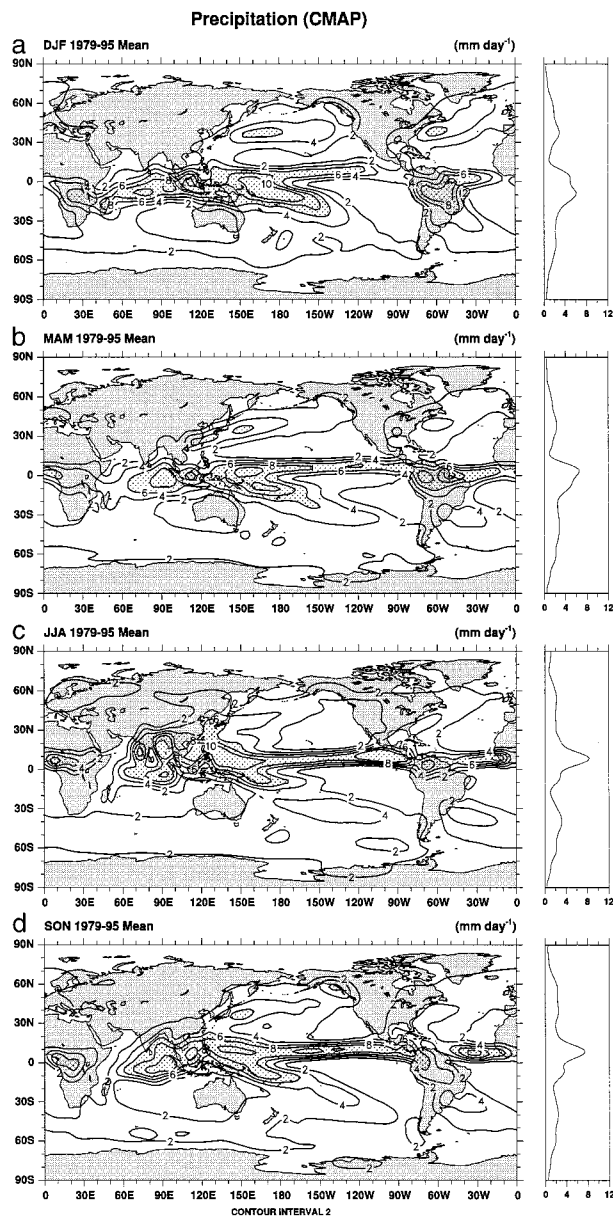


FIG. 1. Seasonal mean precipitation from the Xie-Arkin product for 1979-95 in  $\text{mm day}^{-1}$ . All quantities have been truncated to T31 for presentation in all figures, the contour interval is given below each plot, and the units are at upper right. At right the zonal mean meridional profile is given. Values exceeding  $6 \text{ mm day}^{-1}$  are stippled.

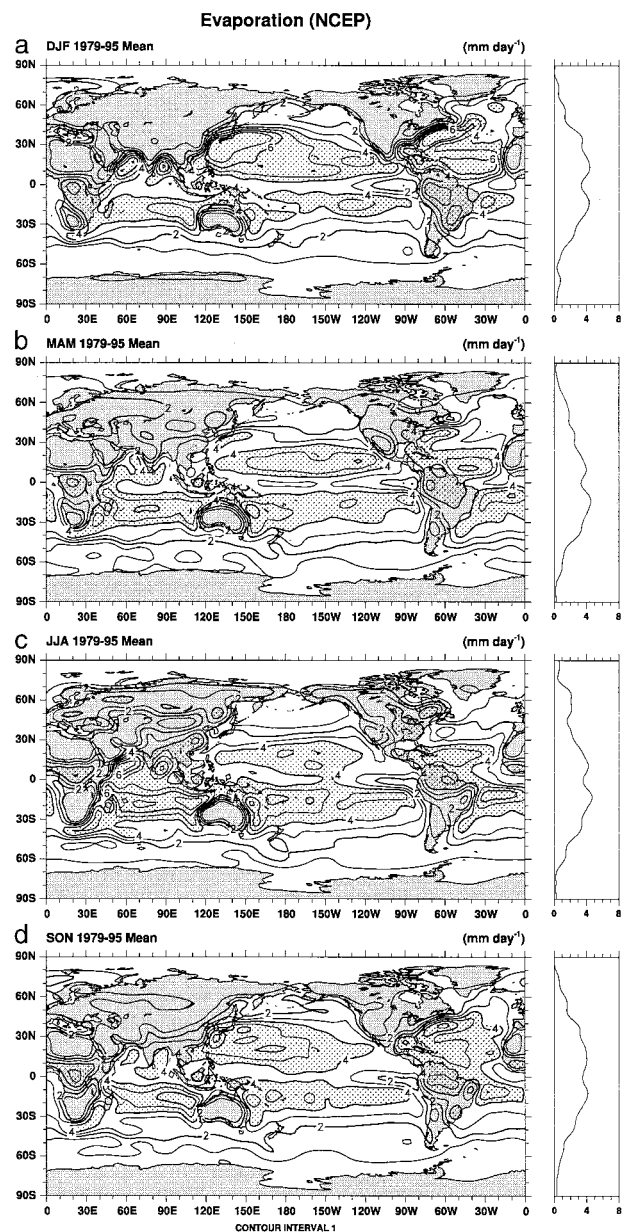


FIG. 2. Seasonal mean evaporation from 1979 to 1995 from the NCEP reanalyses, based upon 6-h model integrations with the assimilating model. Units are  $\text{mm day}^{-1}$ . Values exceeding  $4 \text{ mm day}^{-1}$  are stippled.

reveals strong structures that delineate the land-sea differences as a ready source of moisture. This is especially so in northern winter (December-February, DJF) where cold dry continental air in the Northern Hemisphere flowing over relatively warm oceans produces large evaporative fluxes into the atmosphere. Evaporation rates are typically small ( $<1 \text{ mm day}^{-1}$ ) over land in winter but apparently can exceed  $4 \text{ mm day}^{-1}$  in summer.

As noted above, the moisture available locally for

precipitation depends a great deal on the transport of moisture by the atmosphere from other regions, and the recycling fraction depends on the magnitude of the total moisture flux (Fig. 3). Note that this vertically integrated total includes contributions from the mean flow as well as the high-frequency transient eddies. It is noteworthy that the main moisture transports are east-west, with strong westward components in the Tropics and eastward components in the middle latitudes, but the meridional components linking the two are much weaker. The main exception occurs in June-August (JJA) during

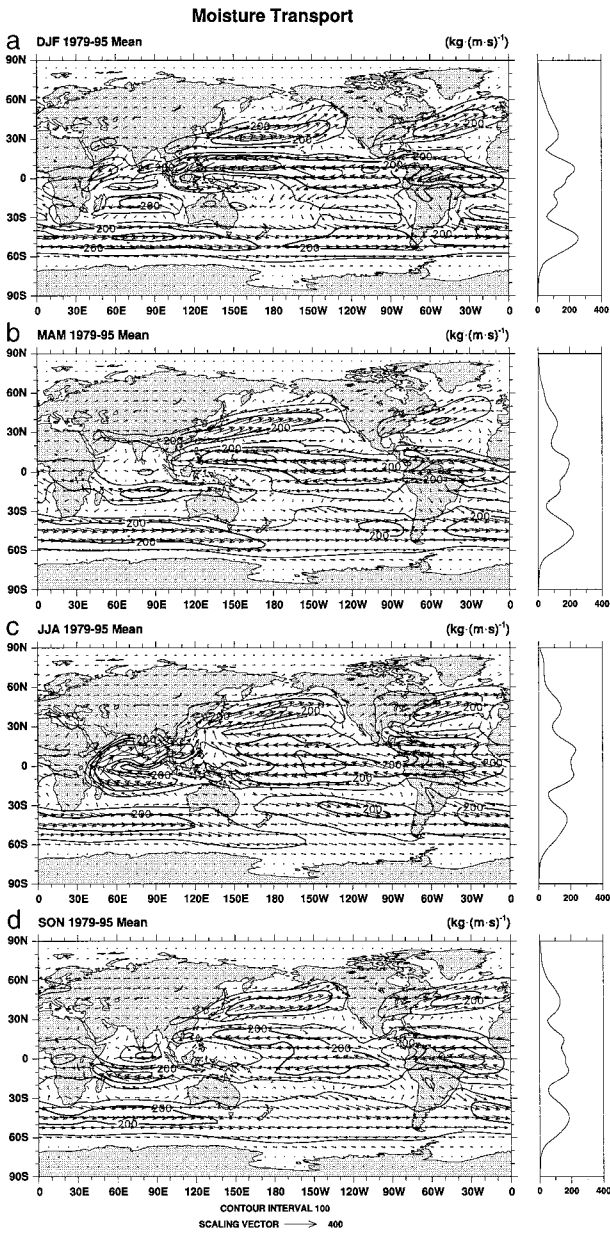


FIG. 3. The seasonal mean moisture transport from the NCEP re-analyses for the period 1979-95. The scale of the vectors is given below and contours indicate magnitudes in kg (m s)<sup>-1</sup>.

the Asian summer monsoon when there is a strong northward flow from the Southern Hemisphere subtropics in the Somalian jet into India and southeast Asia. The corresponding northward flow in the low-level jet from the Gulf of Mexico into the United States is quite small by comparison. The only other meridional moisture flux of consequence is just off the east coast of Brazil in the southern summer. The subtropical highs form the zones between the main zonal transports and are the main sources of evaporation, especially in the winter. The poleward component in the westerlies of

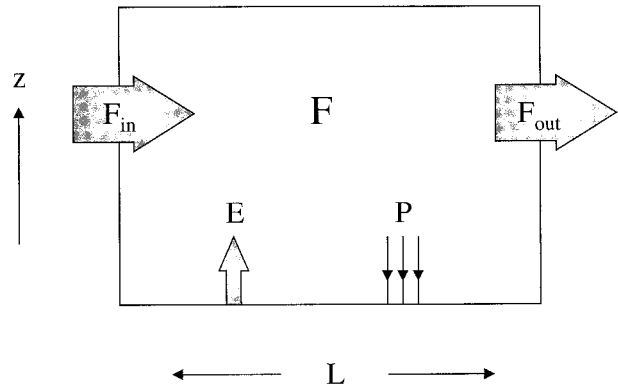


FIG. 4. Schematic for the processes considered in recycling of moisture.

both hemispheres arises mainly from the transient eddy transports associated with baroclinic weather systems.

#### 4. Recycling of moisture

We have computed approximate values of recycling following the approach of Brubaker et al. (1993). Eltahir and Bras (1994, 1996) have proposed alternative formulas and estimation procedures, but some of their assumptions seem harder to justify, as discussed below in this section. Equilibrium conditions are assumed in which there are no changes in atmospheric moisture content. As discussed below, this assumption can be relaxed, but for the results presented here the effects are negligible.

Consider a domain of length  $L$  aligned along the trajectory of the air with a flux of moisture into the box of  $F_{in}$  and a flux out of  $F_{out}$  (Fig. 4) and a total evaporation,  $E$ , and precipitation,  $P$ , in the box; then

$$F_{out} = F_{in} + (E - P)L \quad (1)$$

and the average horizontal moisture flux through the box is

$$F = 0.5(F_{in} + F_{out}) = F_{in} + 0.5(E - P)L. \quad (2)$$

If  $P = P_a + P_m$ , where  $P_a$  is the advective component and  $P_m$  is the component of precipitation arising from local evaporation, then the average horizontal flux of advected moisture over the region is  $F_{in} - 0.5P_aL$ , and the average horizontal flux of locally evaporated moisture is  $0.5(E - P_m)L$ .

An important assumption is that the atmosphere is well mixed so that the ratio of precipitation that falls arising from advection versus local evaporation is equal to the ratio of average advected to evaporated moisture in the air. Thus,

$$\frac{P_a}{P_m} = \frac{F_{in} - 0.5P_aL}{0.5(E - P_m)L}, \quad (3)$$

which is readily solved to give  $P_a/P_m = 2F_{in}/EL$  so that the recycling ratio  $\rho$  can be written

$$\rho = \frac{P_m}{P} = \frac{EL}{EL + 2F_{in}} \quad (4)$$

or, using (2),

$$\rho = \frac{EL}{PL + 2F} \quad (5)$$

This expression involves several other quantities that are of interest. The fraction of water vapor over a region that participates in the hydrological cycle,

$$I = \frac{PL}{F}, \quad (6)$$

has been called the intensity of the hydrological cycle by Drozdov and Grigor'eva (1965), although a more descriptive term might be the precipitation efficiency, as noted earlier. Similarly, we can define a moistening efficiency,

$$M = \frac{EL}{F}, \quad (7)$$

as the fraction of moisture added. Then from (5),

$$\rho = \frac{M}{2 + I}. \quad (8)$$

This formulation has an advantage in that it can be evaluated locally, although formally the results apply to an area with a scale,  $L$ . All of these expressions for  $I$ ,  $M$ , and  $\rho$  depend upon  $L$ . For example, if  $F_{in}$  is  $150 \text{ kg m}^{-1} \text{ s}^{-1}$  and  $E$  is  $4 \times 10^{-5} \text{ kg m}^{-2} \text{ s}^{-1}$  (about  $3.5 \text{ mm day}^{-1}$ ), then  $\rho$  changes from about 1.3% for  $L$  of 100 km to 11.8% for  $L$  of 1000 km. Figure 5 shows some values of  $\rho$  as functions of  $F_{in}$  and  $E$ , for  $L$  of 100 and 1000 km. For small  $E$  (compared with the advective flux),  $\rho$  increases linearly with  $L$ . Note also from (5) that as  $F \rightarrow 0$  then  $\rho = E/P$ .

We have computed results using the full resolution of the datasets available (T62 for the NCEP reanalyses) for length scales  $L$  of 500 and 1000 km. Global annual mean values for the former are also given in Trenberth (1998). While interest has often been on estimates of  $\rho$  for large drainage basins, the heterogeneity of the land surface is such that the recycling clearly varies substantially over the basins. All the computations were done locally in terms of  $I$  and  $M$  and have been smoothed to a T31 resolution for presentation purposes.

The above formulas are approximate, as they assume uniformity that does not exist in practice, and Eqs. (1) and (2) do not hold exactly for the datasets that we have. Clearly, some of the assumptions made above are questionable. A critical assumption in this formulation is that the overall flux of moisture is represented by the mean. The computed flux includes contributions from transients and the mean flow, but the temporal variability of the flux, especially its direction, is not included. Brubaker et al. (1993) also discuss the shortcomings in their formulation and note that "correlations

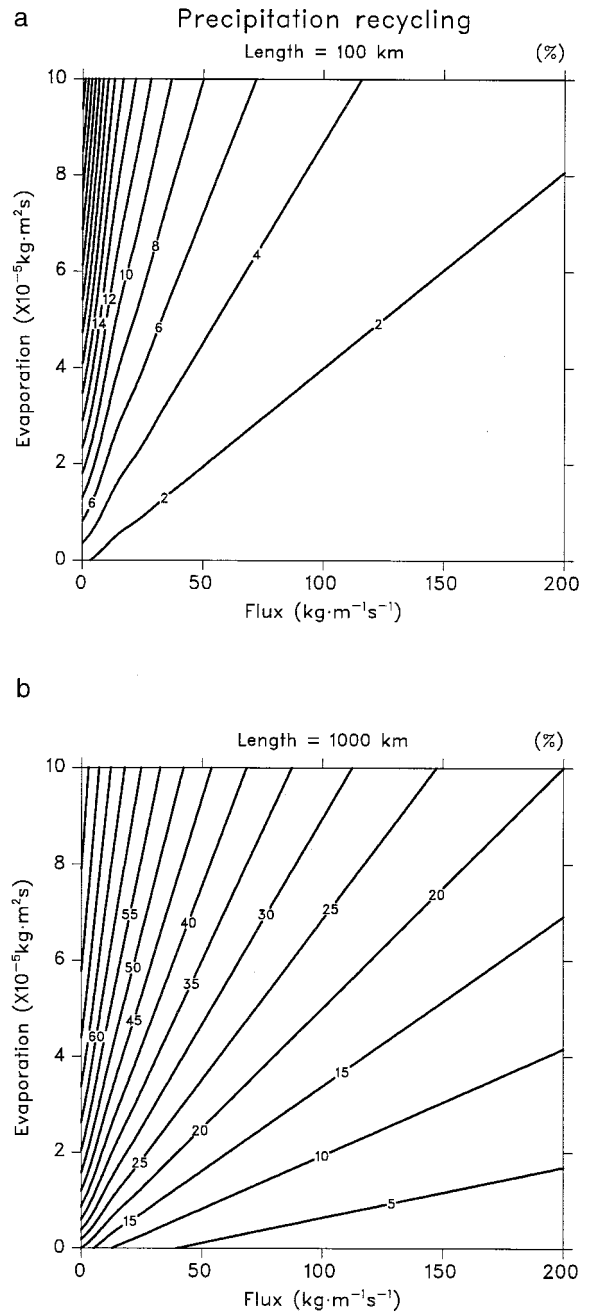


FIG. 5. Values of the recycling percentage as a function of the flux of moisture into a box vs evaporation within the box according to (4) for length scales of 100 and 1000 km.

among the time-varying direction and water content of incoming air masses and precipitation and evaporation rates are neglected."

Some checks have been made on the nonlinearities with temporal variability by making computations for shorter timescales and comparing the results. The effects of these kinds of transients can be seen from (8) if we consider perturbations in the denominator  $I = \bar{I} + I'$ ,

where the overbar indicates a time average. Perturbations in  $M$  are more linear and of less concern. Then, using a binomial expansion and defining  $d' = I'/(2 + \bar{I})$ ,

$$\rho_p = \bar{\rho}(1 + \overline{d'^2/2} \dots), \quad (9)$$

where  $\rho_p$  now includes the effects of perturbations. The last term arises in practice especially from perturbations in precipitation and is positive; thus,  $\rho_p$  is usually somewhat greater than  $\bar{\rho}$ . This has been confirmed by computing  $\rho$  for a season of 90 days and comparing it with  $\rho$  computed for 15- and 30-day periods then averaged to obtain the equivalent seasonal mean value. The latter  $\rho$  is larger by about 0.6% for monthly and 1.4% for 15-day timescales (vs typical values of  $\rho$  of 10%) but with a fairly uniform change so that the pattern changes little. This is a strong test, as a 15-day period is short enough that it may often contain no rainfall at all, so that the recycling of precipitation becomes undefined, as there is *none* to recycle. The discontinuous nature of precipitation probably introduces the greatest transient effects. It is not clear that the values derived from including higher frequencies are superior.

Another indication that these nonlinearities may not be a major consideration comes from results of the International Satellite Land Surface Climatology Project and from the First ISLSCP Field Experiment in particular, which have shown that scaling of several variables, such as evapotranspiration, from local up to large scales, works quite well to enable the calculation of large-scale surface fluxes to acceptable accuracies (e.g., Sellers et al. 1992; Sellers et al. 1997). In other words, effects of topography and the surface radiation budget are near linear and, thus, scale invariant, allowing coarse resolution data to be used to calculate fluxes.

However, it is apparent that some caution is necessary in dealing with the results that should not be taken too literally, and it may therefore be more appropriate to think of  $\rho$  as an index of recycling. Nevertheless, the computation itself is rigorous in deriving a parameter relevant to the hydrological cycle, and results allow different regions of the globe to be compared.

Shortcomings also exist in other approaches to this problem. In Eltahir and Bras (1994), the recycling  $\rho = P_w/P$  is also assumed to be equal to  $O_w/O$ , where  $O$  is the total outflow of moisture and  $O_w$  is the outflow of moisture evaporated within the domain. Although this assumption is built into their computations, it is clearly not satisfied when averaged over the basin (e.g., in their Fig. 12). Thus, there are nonlinearities that arise according to how averages are taken in both space and time. The spatial heterogeneity of the land surface characteristics has led us to focus on the results for 500-km scales.

The above assumed no change in moisture storage in the atmosphere. It is easy enough to allow for moisture changes in (1) and (2), but assumptions such as those in formulating (3) are still necessary. The changes in

storage of atmospheric moisture are systematic with the seasons and are largest for the transition seasons March–May (MAM) and September–November (SON; Trenberth and Guillemot 1996, 1998) but still only amount to about  $0.1 \text{ mm day}^{-1}$ , which is negligible compared with other terms for our current purposes (cf. with Figs. 1 and 2). Because the annual cycle is so important and results vary so much with season, we present results for the individual seasons.

## 5. Results and discussion

While the ratio of local to remote sources of moisture for precipitation is of interest everywhere, the whole concept of recycling is most useful over land where moisture for evaporation is limited by the precipitation, whereas over the oceans the surface is wet regardless of whether it rains or not. Therefore, for several plots we have screened out values over the oceans to focus attention on the land watersheds. We have also screened out regions of mountains (where surface pressures are less than 800 mb) from the calculation, as those are regions where the moisture flux is small and there are huge variations over short distances owing to orographic effects on rainfall. This includes most of Antarctica, and results are not shown poleward of  $50^\circ\text{S}$  and  $75^\circ\text{N}$  because values of  $w$ ,  $P$ , and  $E$  are all very small and not particularly reliable.

The results for the intensity  $I$  for each season (Fig. 6) naturally follow precipitation fields to some extent. Values exceed 40% over the tropical African monsoon region, and migrate back and forth across the equator. Over South America, such high values are apparent only over the southern part of the Amazon Basin, as the large moisture transports over the northern regions (Fig. 3) substantially reduce the ratio of precipitation to transport, especially in the main rainy season of DJF. Other large values of  $I > 40\%$  occur in the convergence zone over the Maritime Continent and thus extend over northern Australia and the Indonesian islands in DJF and migrate to Asia later in the year. Over India, peak  $I$  occurs in SON and not when the rainfalls are at a maximum owing to the strong low-level eastward moisture transports in summer. Seasonal variations over North America and Europe are fairly small. For annual means (Fig. 9), largest intensity occurs over the Maritime Continent in the tropical west Pacific. Values are also large over eastern Siberia, southern Brazil, and northeastern Australia, where annual mean moisture transports are very small. Thus, large intensity can sometimes arise from large precipitation rates but more likely stems from relatively low moisture transports in the atmosphere.

There is a huge annual cycle to the moistening  $M$  (Fig. 7), with maximum values over land occurring over Asia and northwest Canada in northern summer and shifting to tropical Africa and South America south of the equator in the southern summer. Some features of high  $M$  coincide with those of high  $I$  because of their

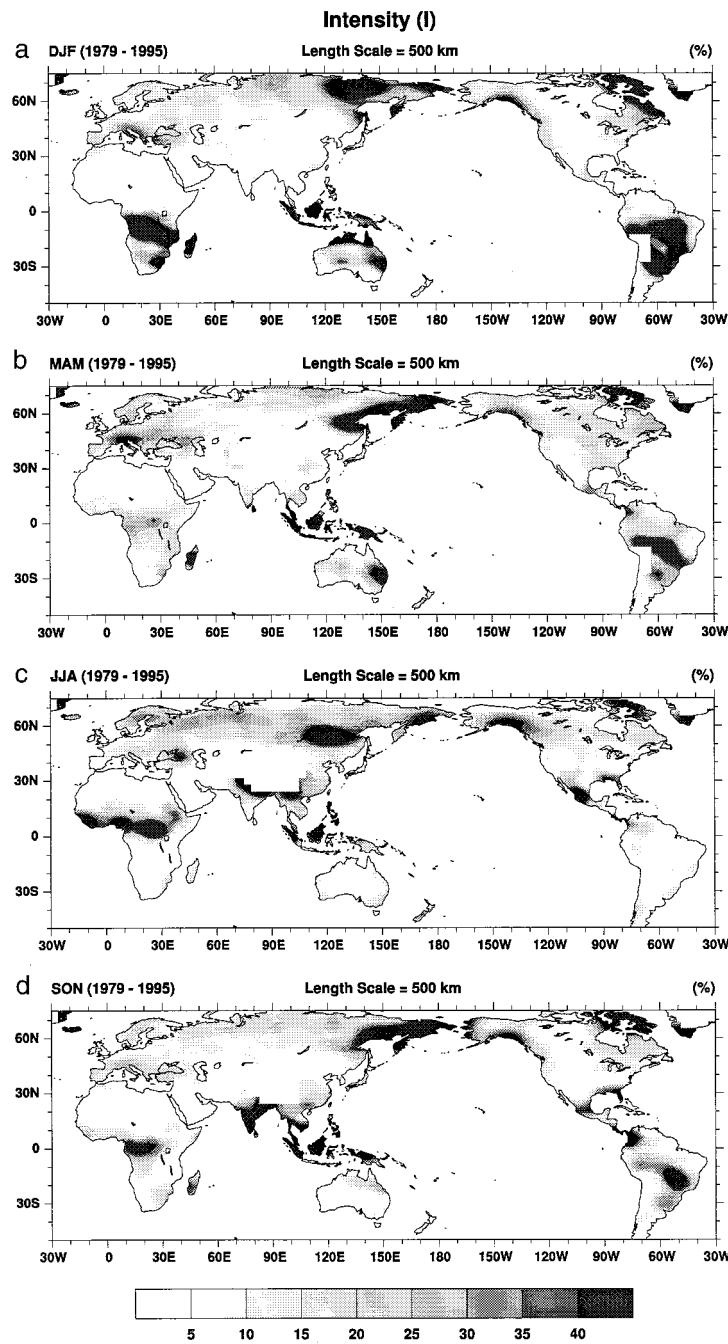


FIG. 6. The intensity of the hydrological cycle  $I$  for the seasonal means computed from (7) for  $L = 500$  km, and using CMAP  $P$  and  $F$  from the NCEP reanalyses.

common factor in the denominator of small moisture transports. This is especially true for the annual means (Fig. 9).

Because  $I$  is mostly in the range of 0%–50%, it is relatively small compared with the factor 2 in (8) and, consequently, the recycling  $\rho$  patterns look very much like those of  $M$  with the magnitude diminished by values of just over 2. As  $L$  increases, however, both  $M$  and  $I$

increase, and then the correspondence between  $M$  and  $\rho$  diminishes somewhat.

The recycling  $\rho$  (Fig. 8) most notably exceeds 16% for 500-km scales throughout much of Siberia as well as northwest Canada in JJA, which is the summer season when potential evapotranspiration is high. These results therefore depend upon the evaporation estimates from NCEP and, because the moisture budget in the analyses

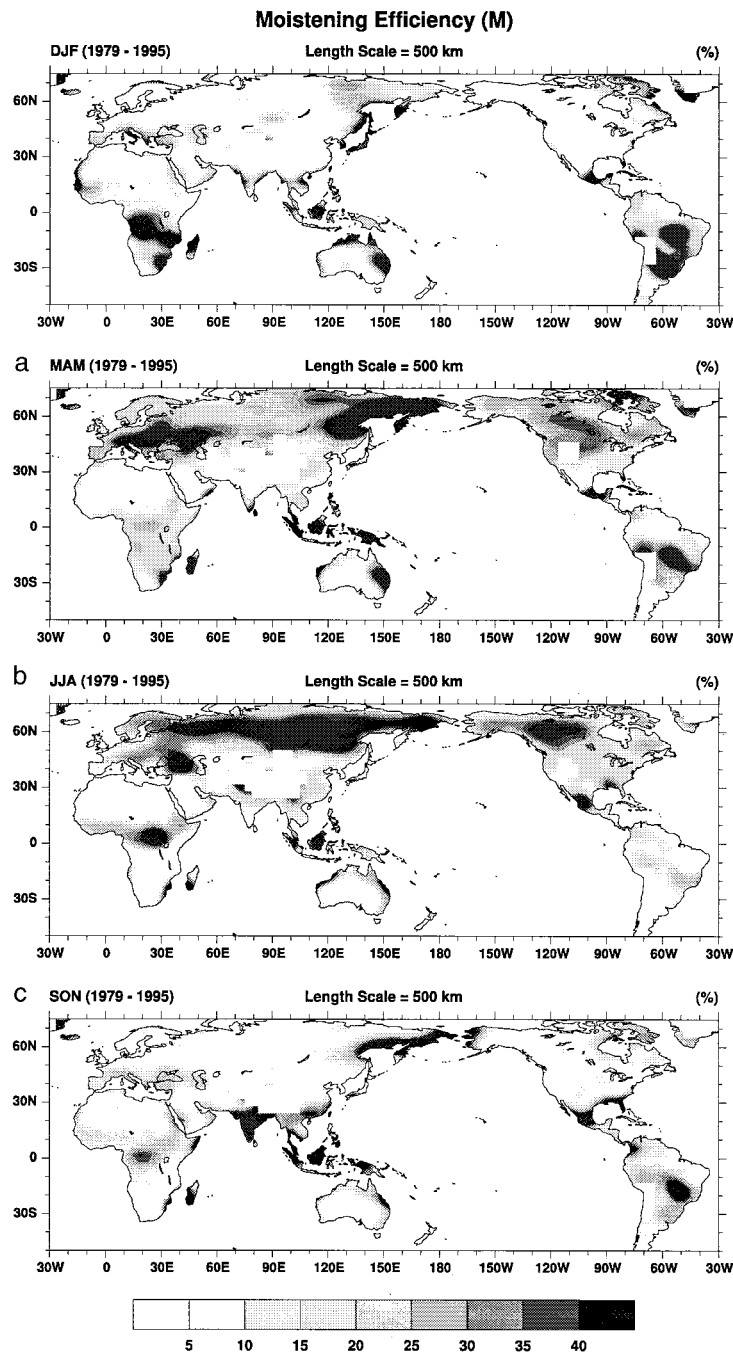


FIG. 7. The moistening efficiency  $M$  for the seasonal means computed from (8) for  $L = 500$  km, and using  $E$  and  $F$  from the NCEP reanalyses.

is not closed (Trenberth and Guillemot 1998), the results need to be checked with other data. Over Africa, maximum values of 12%–20% migrate back and forth across the equator with the convergence zone of maximum precipitation. Maxima over Australia occur in eastern areas in the southern summer (DJF) and autumn (MAM) when moisture transports are smallest in the region.

Very large moisture transports over northern parts of

South America limit  $\rho$  there to values mostly less than 10%. Larger values of  $\rho$  are found south of 10°S in all seasons except southern winter (JJA). Similarly, over India, maximum  $\rho$  occurs in SON, corresponding to the maximum in  $M$ , whereas during summer the monsoon rains are evidently dominated by moisture transported in from the Southern Hemisphere and average  $\rho$  in JJA is about 5%, although it increases northward. In winter

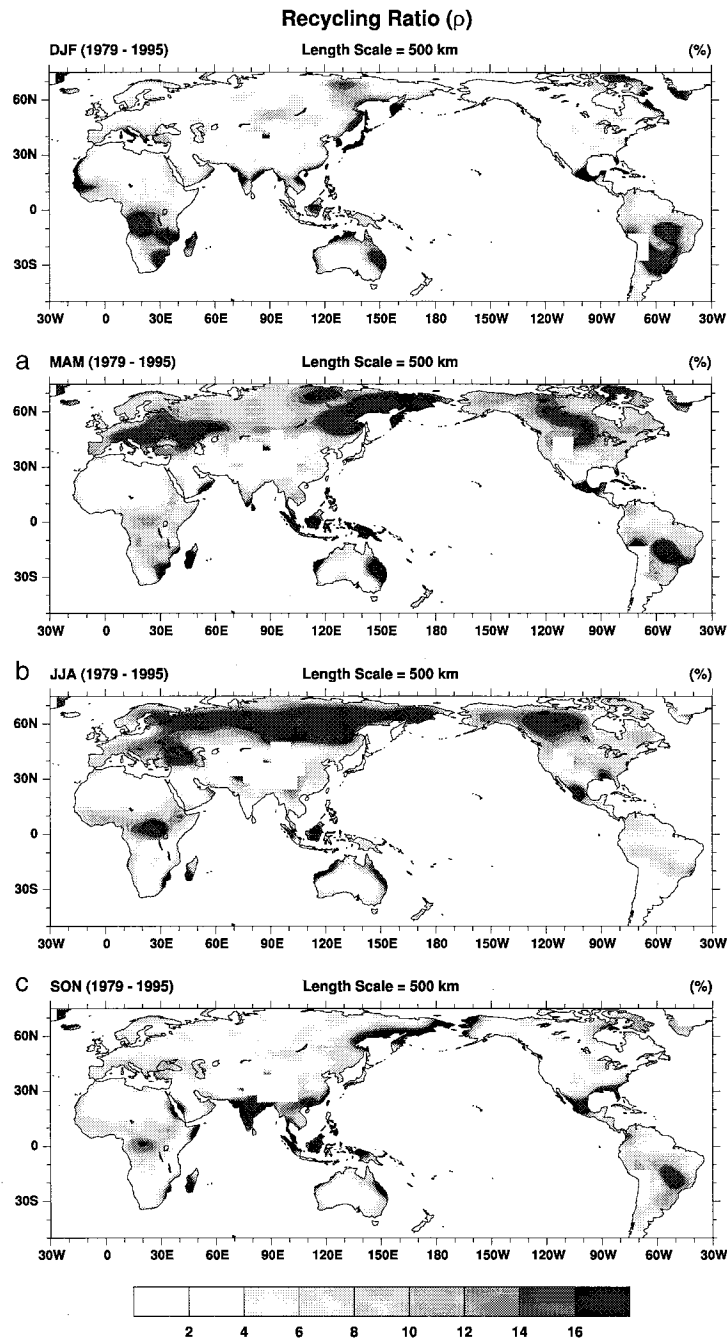


FIG. 8. The recycling (%) for seasonal mean conditions, computed from (5) for  $L = 500$  km, and using  $E$  and  $F$  from the NCEP reanalyses (Figs. 2 and 3) and  $P$  from CMAP (Fig. 1).

over the northern continents  $\rho$  drops to less than 5% over most regions, reflecting the low potential evapotranspiration and tendency for most moisture that is precipitated to be transported into the region in transient extratropical storms.

For the annual mean at 500 km (Fig. 9),  $\rho$  varies from almost zero over the main deserts of Africa, Australia,

and parts of Asia to over 16% in northeast Siberia and the Maritime Continent. Values are close to 8% over northern Asia from 30° to 100°E, and increase from less than 4% over northern Europe to >12% over the Mediterranean coast. Values of  $\rho$  are about 7% for annual means over the Mississippi Basin and increase to just over 10% in the MacKenzie Basin. Substantial gradients

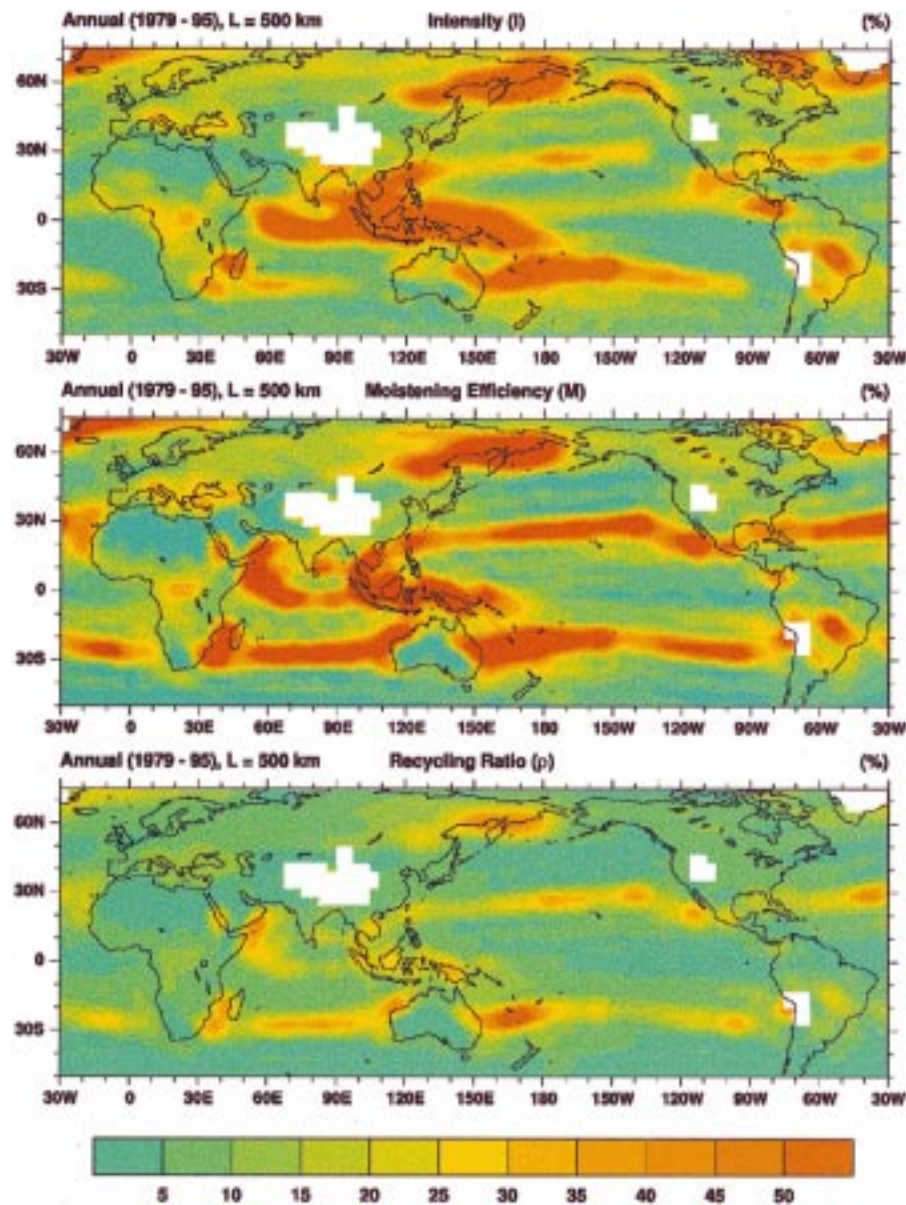


FIG. 9. For annual mean conditions, given are  $I$ ,  $M$ , and the recycling  $\rho$  in percent for  $L = 500$  km, using  $E$  and  $F$  from the NCEP reanalyses (Figs. 2 and 3) and  $P$  from CMAP (Fig. 1).

exist over the Amazon River Basin from over 15% in the south to about 5% over the equatorial regions.

It is apparent that values for recycling vary substantially with the seasons when the formulas are applied with seasonal mean data. To determine seasonal mean values, the numerators of  $I$ ,  $M$ , and  $\rho$  were obtained by computing weighted (by number of days per season) averages of the seasonal values of  $E$  or  $P$ . The corresponding denominators were obtained by computing weighted averages of seasonal values of  $F$  (and  $P$  in the case of  $\rho$ ). To further establish the degree to which temporal averaging affects the results, the weighted averages of the seasonal values of  $I$ ,  $M$ , and  $\rho$  are compared

with their annual mean counterparts. Because  $F$  appears in the denominators of (5), (6), and (7), it was suspected that large magnitudes of  $F$  could arise in one season and distort the seasonal average but have little influence on the annual mean. The differences turn out to be remarkably small ( $<3\%$ ) with an exception for  $M$  in northeastern Siberia where the differences are about 6%. For recycling, the differences are mostly within  $\pm 1\%$ .

The recycling results for annual means (Fig. 9) reveal recycling percentages for 500-km scales of about 5%–10% over land typically. The global mean is 9.6%, consisting of 8.9% over land and 9.9% over the oceans. For 1000-km scales (Fig. 10)  $\rho$  is about 8%–20% over land

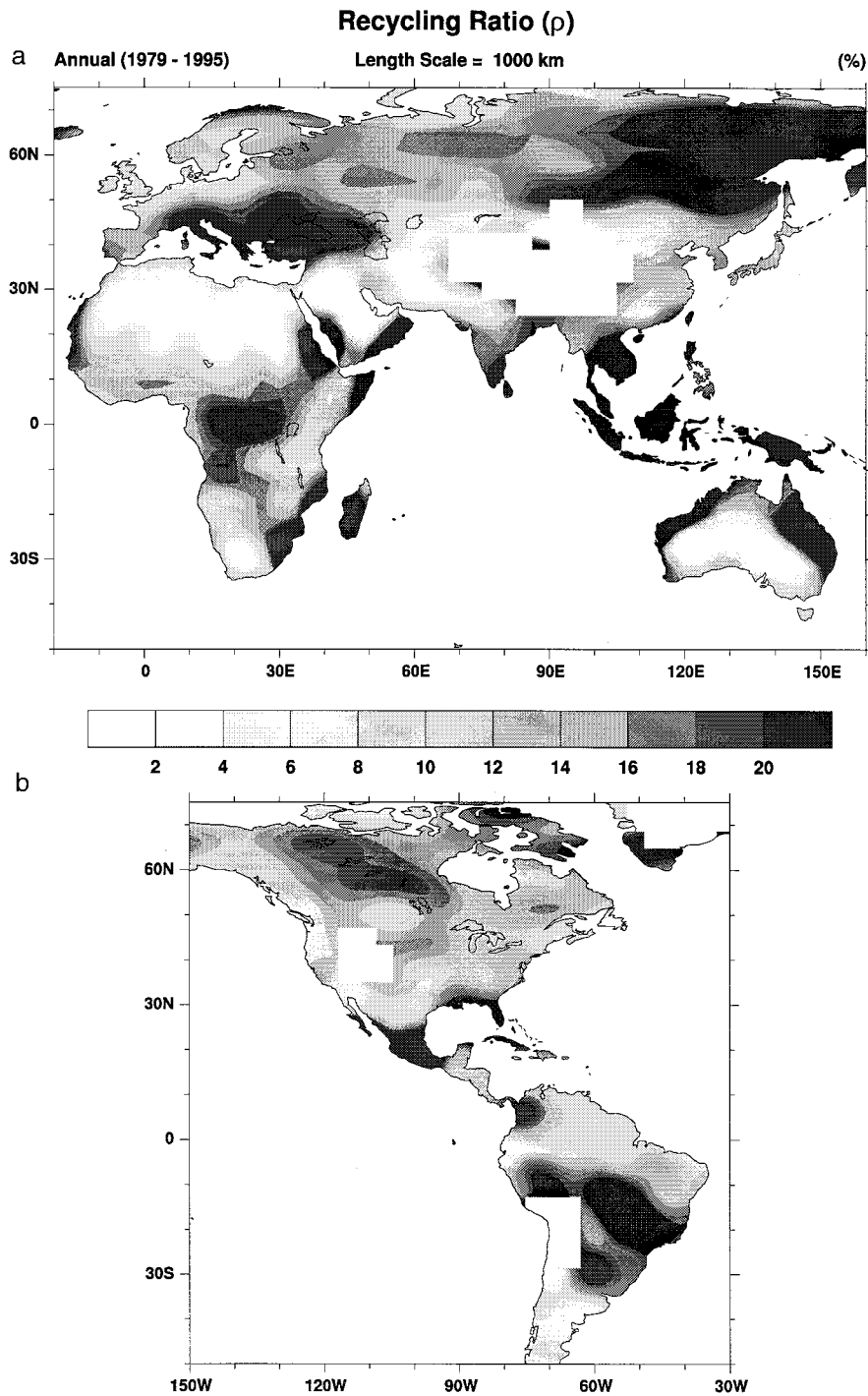


FIG. 10. For annual mean conditions,  $\rho$ , the recycling (%) for  $L = 1000$  km over land.

typically and the mean recycling is 16.8% globally, 15.4% over land and 17.3% over the oceans.

Over the Amazon, the results depend greatly upon whether or not the maximum over the southern part of the basin, where  $\rho > 20\%$ , is included. The South American region defined by Brubaker et al. (1993) is from

2.5°N to 15°S, 50° to 75°W (which is a reasonable approximation of the Amazon River Basin), for which the average annual recycling on 500-km scales is 8.7%, ranging from 5.7% in JJA to 11.9% in DJF. But if the region is cut off at 10°S, the values drop to 6.4% for the annual mean and with a range of 4.8% in JJA to

7.7% in DJF. For the full basin over the length scale of 2750 km, the Amazon annual average recycling is about 34%. Here, use was made of the mean  $E$ ,  $P$ , and  $F$  over the basin and (6), scaled to match the result at 500 km. For the Mississippi Basin, which Brubaker et al. (1993) define to be 32.5°–42.5°N, 85°–105°W, the average recycling at 500-km scales is 6.6%, ranging from 3.1% in DJF to 9.3% in JJA. Converting to the length scale of 1800 km, the annual recycling is about 21%. Thus, our results are not incompatible with the 25%–35% recycling (e.g., Eltahir and Bras 1994; Brubaker et al. 1993) obtained by previous studies in the Amazon and a monthly mean of 24% from Brubaker et al. (1993) in the Mississippi Basin. It is worth pointing out that the larger values previously obtained for the Amazon versus the Mississippi are mostly a result of the scale of the domain because over much of the basin the recycling fraction is actually less.

Relatively high annual values (>20%) of recycling occur both in the subtropical highs, where  $E$  is high and the advective moisture flux is small, and in convergence zones where, again, the advective moisture flux is small (Fig. 3). This may be somewhat misleading, as the very nature of the convergence zones implies that it is the convergence of moisture by the low-level winds that is dominant. In such regions, referring back to Fig. 4,  $F_{in} \sim -F_{out}$ , yet both  $F_{in}$  and  $F_{out}$  can be large. Thus, the finite size of the domain is important and the use of (4) in place of (5) would change the results in these regions. Low annual values of  $\rho$  occur over the southern oceans, the North Pacific, and the eastern equatorial Pacific, where the moisture flux is at a maximum (Fig. 3).

## 6. Conclusions

An approximate formulation for recycling has been developed that allows new estimates to be mapped globally as a function of length scale of the domain (which might correspond to a river basin, for instance). The recycling is formulated in terms of the intensity of the hydrological cycle (also known as the precipitation efficiency) and the moistening efficiency, which, respectively, measure the relative contributions of precipitation and evaporation to the atmospheric moisture flux as sources or sinks of moisture.

As discussed earlier, computation of recycling empirically requires assumptions that suggest that the results should not be taken too literally. A test of the assumptions involving temporal variability, which are probably most critical, has been made by comparing the mean of four seasonal values with the results computed for the annual mean, indicating only very small (mostly less than 3%) effects; further tests using subdivided data indicate that values may be underestimated somewhat, but the patterns are quite robust. Therefore, it is suggested that it is more appropriate to think of these results as providing an index of recycling, which does allow

different regions of the globe to be compared under the assumptions made.

One important conclusion of note is that, often, the intensity of the hydrological cycle, as defined, is not necessarily greatest at times of greatest precipitation because that is often also the time of greatest moisture transport, especially in the monsoonal regions. The annual cycle variations of  $I$  are fairly small over North America and Europe whereas large seasonal variations in  $M$  occur in most places.

It is apparent that the recycling results depend greatly on the scale of the domain under consideration and that heterogeneity is generally present over land, so that average recycling values for a particular region are often composed of very disparate components. Over the Amazon, for instance, strong advection of moisture dominates the supply of atmospheric moisture over much of the domain but local evaporation is much more prominent over the southern parts. The values of recycling over the main river basins will depend on the exact borders used to define the domain. Using the simplified rectangular domains of Brubaker et al. (1993), it is estimated that over the Amazon, for the annual cycle as a whole, about 34% of the moisture is recycled. Over the Mississippi Basin the recycling is about 21%, slightly smaller than the estimate of Brubaker et al. It is important to note that the recycling per unit area is greater over the Mississippi than most of the Amazon Basin; the above result depends on the domain size and on the high values of recycling over the southern parts of the Amazon Basin. Also, the exact numbers will change if more realistic borders are used.

The global maps of the recycling for seasonal and annual means on 500- and 1000-km scales reveal the heterogeneity of the fields across watersheds and river basins. Global annual mean recycling on 500-km scales is just less than 10% but varies greatly over land from less than 2% to over 20%, and with values slightly less than doubled for 1000-km scales. The annual cycle is large, not unexpectedly, as the potential evapotranspiration peaks in summer, while advection and atmospheric dynamics are more prominent in winter.

The computations of recycling and the related quantities presented here depend on the quality of the datasets used. These were discussed in section 2, and while some problems were noted, the data are believed to be better than used in previous estimates of global hydrological variables of interest. Consequently, the details of the results need to be checked with other datasets. In particular, results that depend upon evaporation over continents in winter and the divergent atmospheric circulation (such as in the moisture convergence in the atmosphere) may be subject to revisions, although it is anticipated that the broadscale aspects should remain credible. The general conclusions given are believed to be robust to the data problems, although quantitative values are open to revision in detail.

It is not clear how the recycling estimates could be

greatly improved through the kind of empirical approach used here because a number of assumptions appear to be necessary. In a climate model it would be possible in principle to label each parcel of atmospheric moisture with its source and age, and trace each parcel to wherever it is precipitated (Jousaume et al. 1986; Koster et al. 1986). While potentially quite enlightening, this approach also makes assumptions concerning subgrid-scale mixing, diffusion, and precipitation processes, such as convection parameterization, and depends on the fidelity of the simulation. Thus far, simulations of convection do not match observations adequately to have complete confidence in this approach (e.g., Dai et al. 1999). Nevertheless, the method has different assumptions and, thus, is complementary.

Finally, it should be noted that the dominance of the moisture transport in feeding the Amazon rains and monsoonal rains in many other areas seems to imply that sensitivity to changes in land surface characteristics would be reduced were this not the case. Of course, changes in vegetation that produce even small changes in evaporation and moisture availability may still be sufficient to alter the precipitation, latent heating, and, thus, atmospheric circulation and moisture transport, which means that this line of argument *should not be pushed very far*. The strongly nonlinear feedbacks can only be captured in a comprehensive climate model.

*Acknowledgments.* This research is partly sponsored by NOAA under Grant NA56GP0247 and by a joint NOAA/NASA grant (NA56GP0576). I thank David Stepaniak and Chris Guillemot for performing the computations and producing the figures.

#### REFERENCES

- Arkin, P. A., and P. Xie, 1994: The Global Precipitation Climatology Project: First algorithm intercomparison project. *Bull. Amer. Meteor. Soc.*, **75**, 401–419.
- Brubaker, K. L., D. Entekhabi, and P. S. Eagleson, 1993: Estimation of continental precipitation recycling. *J. Climate*, **6**, 1077–1089.
- Dai, A., F. Giorgi, and K. E. Trenberth, 1999: Observed and model simulated precipitation diurnal cycles over the contiguous United States. *J. Geophys. Res.*, in press.
- Drosdov, O. A., and A. S. Grigor'eva, 1965: *The Hydrologic Cycle in the Atmosphere*. Israel Program for Scientific Translations, 282 pp.
- Eltahir, E. A. B., and R. L. Bras, 1994: Precipitation recycling in the Amazon basin. *Quart. J. Roy. Meteor. Soc.*, **120**, 861–880.
- , and —, 1996: Precipitation recycling. *Rev. Geophys.*, **34**, 367–378.
- Fankhauser, J. C., 1988: Estimates of thunderstorm precipitation efficiency from field measurements in CCOPE. *Mon. Wea. Rev.*, **116**, 663–684.
- Ferrier, B. S., J. Simpson, and W.-K. Tao, 1996: Factors responsible for precipitation efficiencies in midlatitude and tropical squall simulations. *Mon. Wea. Rev.*, **124**, 2100–2125.
- Huffman, G. J., and Coauthors, 1997: The Global Precipitation Climatology Project (GPCP) combined precipitation dataset. *Bull. Amer. Meteor. Soc.*, **78**, 5–20.
- Jousaume, S., R. Sadourny, and C. Vignal, 1986: Origin of precipitating water in a numerical simulation of the July climate. *Ocean–Air Inter.*, **1**, 43–56.
- Kalnay, E., and Coauthors, 1996: The NCEP/NCAR 40-Year Reanalysis Project. *Bull. Amer. Meteor. Soc.*, **77**, 437–471.
- Koster, R. D., J. Jouzel, R. Suozzo, G. Russell, W. Broecker, D. Read, and P. S. Eagleson, 1986: Global sources of local precipitation as determined by the NASA/GISS GCM. *Geophys. Res. Lett.*, **13**, 121–124.
- Randel, D. L., T. H. Vonder Haar, M. A. Ringerud, D. L. Reinke, G. L. Stephens, T. J. Greenwald, and C. L. Combs, 1996: A new global water vapor dataset. *Bull. Amer. Meteor. Soc.*, **77**, 1233–1246.
- Sellers, P. J., M. D. Heiser, and F. G. Hall, 1992: Relations between surface conductance and spectral vegetation indices at intermediate (100 m<sup>2</sup> to 15 km<sup>2</sup>) length scales. *J. Geophys. Res.*, **97**, 19 033–19 059.
- , —, —, S. B. Verma, R. L. Desjardins, P. M. Schuepp, and J. I. MacPherson, 1997: The impact of using area-averaged land surface properties—topography, vegetation condition, soil wetness—in calculations of intermediate scale (approximately 10 km<sup>2</sup>) surface-atmosphere heat and moisture fluxes. *J. Hydrol.*, **190**, 269–301.
- Trenberth, K. E., 1998: Atmospheric moisture residence times and cycling: Implications for rainfall rates and climate change. *Climate Change*, **39**, 667–694.
- , and C. J. Guillemot, 1996: Evaluation of the atmospheric moisture and hydrological cycle in the NCEP reanalyses. NCAR Tech. Note NCAR/TN-430+STR, 300 pp.
- , and —, 1998: Evaluation of the atmospheric moisture and hydrological cycle in the NCEP reanalyses. *Climate Dyn.*, **14**, 213–231.
- Xie, P., and P. A. Arkin, 1996: Analyses of global monthly precipitation using gauge observations, satellite estimates, and numerical model predictions. *J. Climate*, **9**, 840–858.
- , and —, 1997: Global precipitation: A 17-year monthly analysis based on gauge observations, satellite estimates, and numerical model outputs. *Bull. Amer. Meteor. Soc.*, **78**, 2539–2558.